Mathematical and Computer Modelling 50 (2009) 1142–1153

Contents lists available at ScienceDirect

Mathematical and Computer Modelling

journal homepage: www.elsevier.com/locate/mcm

Optimal control of non-isothermal viscous fluid flow☆

C.L. Cox[a,*], H. Lee[a], D.C. Szurley[b]

[a] Department of Mathematical Sciences, Clemson University, Clemson, SC 29634-0975, United States

[b] Department of Mathematics, Francis Marion University, Florence, SC 29501, United States

ARTICLE INFO

Article history:
Received 27 May 2008
Received in revised form 19 December 2008
Accepted 5 June 2009

Keywords:
Optimal control
Stokes–Oldroyd model
Non-isothermal
Viscous flow
Four-to-one contraction
Finite element method

ABSTRACT

For flow inside a four-to-one contraction domain, we minimize the vortex that occurs in the corner region by controlling the heat flux along the corner boundary. The problem of matching a desired temperature along the outflow boundary is also considered. The energy equation is coupled with the mass, momentum, and constitutive equations through the assumption that viscosity depends on temperature. The latter three equations are a non-isothermal version of the three-field Stokes–Oldroyd model, formulated to have the same dependent variable set as the equations governing viscoelastic flow. The state and adjoint equations are solved using the finite element method. Previous efforts in optimal control of fluid flows assume a temperature-dependent Newtonian viscosity when describing the model equations, but make the simplifying assumption of a constant Newtonian viscosity when carrying out computations. This assumption is not made in the current work.

1. Introduction

We consider the four-to-one contraction domain, where a fluid is flowing through a channel whose width is suddenly reduced by three-quarters. This geometry commonly occurs, for example, in the forming 'die' used in extrusion processes. Due to the sudden reduction in width, in the corner region a vortex appears, as in Fig. 1. In this region where the fluid recirculates it has the potential to degrade, which produces an inferior product, for example, in the case of polymer extrusion. Therefore, we would like to be able to control some parameter(s) of the flow to reduce this vortex. We also consider the problem of temperature matching. We wish to match a specified temperature along the outflow boundary, which represents the die exit.

The characteristics of isothermal fluid flows (Newtonian, shear-thinning, and viscoelastic) through a contraction domain are described in [1]. Finite element simulations for isothermal Newtonian and generalized Newtonian fluids through a contraction domain are presented in [2]. For fluid flows involving high viscosities and high deformation rates, non-isothermal effects should not be overlooked, as unexpected consequences are known to occur [3].

Kunisch and Marduel [4] and Ito and Ravindran [5] both consider two-dimensional adjoint-based optimization for non-isothermal flow. Although the fluid in both papers is assumed to be non-isothermal, in both cases the Newtonian viscosity is independent of temperature. Ito and Ravindran consider the Boussinesq viscous flow equations, and hence stress is not an unknown. The focus of that work is minimizing vortices by controlling the temperature along a portion of the boundary. A cost functional is introduced where the curl of the velocity field is minimized over the domain or a portion of the domain. The authors look at the backward-facing-step channel as well as a vertical reactor. It is shown that they can reduce the L^2 norm (squared) of the vorticity by 46% by controlling the temperature along a portion of the boundary.

☆ This work was supported primarily by the ERC program of the National Science Foundation under Award Number EEC-9731680.

* Corresponding author.
E-mail addresses: clcox@clemson.edu (C.L. Cox), hklee@clemson.edu (H. Lee), dszurley@fmarion.edu (D.C. Szurley).

0895-7177/$ – see front matter © 2009 Elsevier Ltd. All rights reserved.
doi:10.1016/j.mcm.2009.06.006

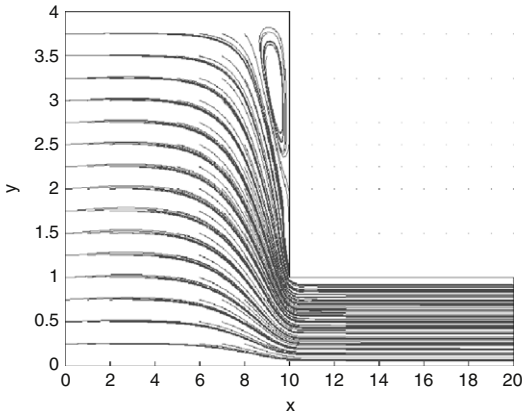

Fig. 1. Typical streamlines of velocity **u**.

In [4] the authors also consider vortex minimization, although there are differences between [4,5], the first of which is the computational domain. In [4], they consider flow of a non-isothermal viscoelastic fluid (governed by the linearized Phan-Thien/Tanner model) through the four-to-one contraction domain. They introduce two cost functionals, both of which are intended to minimize the vorticity. One minimizes the difference between the computed flow field and the flow field of a Newtonian fluid, and the other penalizes negative contributions of the velocity field to prevent recirculation. They do not assume symmetry, and hence apply one cost functional to each corner region. Using temperature as a control, they show that the vortex can be reduced, and then discuss in physical terms what has to happen to lead to a reduction in the vortex.

Like [5,4], we consider non-isothermal flow. However, we do not make the assumption that the Newtonian viscosity is independent of temperature; that is, the energy equation is coupled to the constitutive and momentum equations through the viscosity. Our results indicate that an 80% reduction in the vorticity can be achieved.

The outline of the rest of this paper is as follows. In Section 2 we present the governing equations, with particular attention given to the manner in which temperature dependence is expressed. The optimization problem is defined in Section 3. Section 4 contains details of the weak formulation of the governing equations and the computational algorithm. Numerical results for three model problems are presented in Section 5, and Section 6 contains a summary and a discussion of future work.

2. Governing equations

The current effort is directed towards the long term goal of optimal control of viscoelastic fluid flow. The development of the state equations begins with the governing equations in [6], where the Stokes problem is formulated with the same three-field dependent variable structure as the Maxwell model for viscoelastic flow. We consider fluid flowing through a bounded, connected domain $\Omega \subset \mathbb{R}^2$, with Lipschitz continuous boundary Γ. Let the velocity be denoted by **u**, pressure p, extra stress $\underline{\sigma}$, and temperature T. The isothermal Stokes–Oldroyd equations presented in [6] are

$$\underline{\sigma} - 2\alpha d(\mathbf{u}) = \underline{0} \quad \text{in } \Omega, \tag{1}$$

$$-\nabla \cdot \left[\underline{\sigma} + 2(1-\alpha)d(\mathbf{u})\right] + \nabla p = \mathbf{f} \quad \text{in } \Omega, \tag{2}$$

$$\nabla \cdot \mathbf{u} = 0 \quad \text{in } \Omega. \tag{3}$$

In (1) and (2), $d(\mathbf{u})$ represents the rate of deformation tensor, defined as

$$d(\mathbf{u}) = \frac{1}{2}\left(\nabla \mathbf{u} + (\nabla \mathbf{u})^T\right),$$

and **f** is a body source term. When viscoelastic terms are included in Eqs. (1) and (2), α may be interpreted as the viscoelastic part of the total viscosity. In the Newtonian case, keeping $0 < \alpha < 1$ alleviates the need, in the discrete formulation, for an inf–sup condition on $(\underline{\sigma}, \mathbf{u})$, [6].

We introduce a temperature-dependent viscosity using an Arrhenius relationship, [7], i.e.

$$\eta(T) = A \exp\left(\frac{B}{T}\right). \tag{4}$$

The rheological constants in (4) are determined experimentally as

$$B = \frac{\Delta E}{R}, \qquad A = \eta_0 \exp\left[\frac{-\Delta E}{RT_R}\right],$$

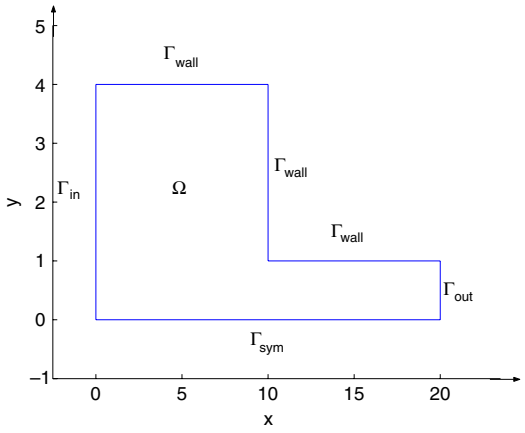

Fig. 2. Computational domain Ω.

where ΔE is the activation energy, R the ideal gas constant, T_R is a reference temperature, and $\eta_0 = \eta(T_R)$, [7]. The Arrhenius relationship is commonly assumed to be applicable for temperatures above $T_g + 100\,^\circ$C, where T_g is the glass transition temperature of the polymer. For $T_g < T < T_g + 100\,^\circ$C, the WLF (Williams–Landel–Ferry) equation is often used. Variation between polymers makes it difficult to establish a rule about which model to use for all cases [8]. Since we are concerned with a molten flow upstream from the quench environment, the Arrhenius model is used in this paper. As in [4,5], we drop the viscous heating term in the energy equation, so that the governing equations are

$$\underline{\sigma} - 2\alpha\eta(T)d(\mathbf{u}) = \underline{0} \quad \text{in } \Omega, \tag{5}$$

$$-\nabla\cdot\left[\underline{\sigma} + 2(1-\alpha)\eta(T)d(\mathbf{u})\right] + \nabla p = \mathbf{f} \quad \text{in } \Omega, \tag{6}$$

$$\nabla\cdot\mathbf{u} = 0 \quad \text{in } \Omega, \tag{7}$$

$$-\nabla\cdot(\kappa\nabla T) + \mathbf{u}\cdot\nabla T = Q \quad \text{in } \Omega, \tag{8}$$

where in (8), κ is a dimensionless term related to thermal conductivity and Q is a heat source term. In light of the earlier discussion, α is included in this formulation. As in (1) and (2), α in (5) and (6) is a constant with $0 < \alpha < 1$. Its role is more numerical than physical. Properties of the weak solution to Eqs. (5)–(8) are analyzed in [9].

As shown in Fig. 2, boundary Γ is divided into four disjoint parts: the inflow boundary Γ_{in}, the wall boundary Γ_{wall}, the outflow boundary Γ_{out}, and the symmetry boundary Γ_{sym} (so that $\Gamma = \Gamma_{\text{in}} \cup \Gamma_{\text{wall}} \cup \Gamma_{\text{out}} \cup \Gamma_{\text{sym}}$). Then the boundary conditions are as follows [10]:

$$\mathbf{u} = \mathbf{u}_{\text{in}}, \qquad T = T_0 \quad \text{on } \Gamma_{\text{in}}, \tag{9}$$

$$\mathbf{u} = \mathbf{0}, \qquad \nabla T\cdot\mathbf{n} = 0 \quad \text{on } \Gamma_{\text{wall}}, \tag{10}$$

$$\mathbf{u} = \mathbf{u}_{\text{out}}, \qquad \nabla T\cdot\mathbf{n} = 0 \quad \text{on } \Gamma_{\text{out}}, \tag{11}$$

$$\mathbf{u}\cdot\mathbf{n} = 0, \qquad \nabla T\cdot\mathbf{n} = 0, \qquad \underline{\pi} : \mathbf{nt} = 0 \quad \text{on } \Gamma_{\text{sym}}. \tag{12}$$

In (12), $\underline{\pi}$ is the Cauchy stress tensor, and unit vectors outward and tangential to the boundary are $\mathbf{n}$ and $\mathbf{t}$, respectively. A double contraction between two second-rank tensors $\underline{\tau}$ and $\underline{\sigma}$ is defined as

$$\underline{\tau} : \underline{\sigma} = \sum_{i,j} \tau_{ij}\sigma_{ji}.$$

Note that the boundary condition $\underline{\pi} : \mathbf{nt}$ on Γ_{sym} is equivalent for the problem considered here to $\frac{\partial u_1}{\partial y} = 0$. A discussion of other outflow boundary conditions can be found in [11].

3. Optimization problem and adjoint equations

As stated previously our goal is to minimize the vortex in the corner region, as shown in Fig. 1, or ideally eliminate it altogether. A measure of the vortex is the curl of the velocity field. Hence, an optimization problem consists of minimizing the magnitude of the curl, e.g.,

$$\int_\Omega (\nabla\times\mathbf{u})^2\,\mathrm{d}\Omega \tag{13}$$

subject to the state equations (5)–(8) with boundary equations (9)–(12). We will also consider matching a desired temperature T^* along the outflow boundary. Then our optimization problem is to minimize a linear combination of the integrals

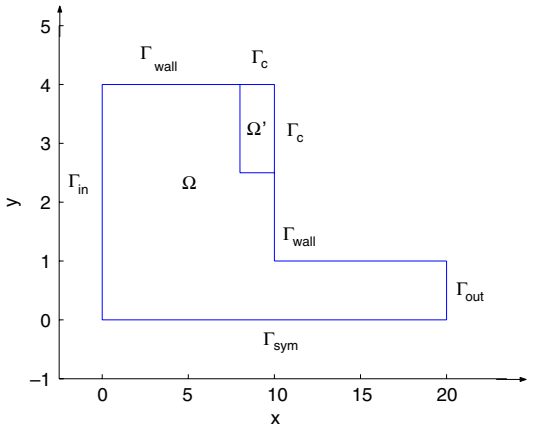

Fig. 3. Domain of the control problem.

$$\int_{\Omega} (\nabla \times \mathbf{u})^2 \, \mathrm{d}\Omega \quad \text{and} \quad \int_{\Gamma_{\text{out}}} (T - T^*)^2 \mathrm{d}\Gamma,$$

subject to (5)–(12).

With the quantity that is to be minimized defined, as well as the constraints, it is now necessary to define the control variable. Similar to Kunisch et al. [4], we consider affecting the flow by a temperature boundary control. However, while the authors of [4] consider temperature T along a portion of the boundary as their control, we consider controlling the heat flux over a portion of the boundary, as in [12], and using a formulation similar to that in [5]. Specifically, we let our control $\tilde{g}$ be defined as

$$\tilde{g} = -\kappa \nabla T \cdot \mathbf{n},$$

which is applied to a subset Γ_c of the boundary, (see Fig. 3). We now have the following conditions on the control boundary Γ_c:

$$\mathbf{u} = \mathbf{0},$$
$$-\kappa \nabla T \cdot \mathbf{n} = \tilde{g},$$

where the quantity $\tilde{g}$ is determined by optimization.

In order to ensure that the control $\tilde{g}$ has a realistic magnitude, we introduce a penalty term. Also, we will weight the curl and temperature integrals in order to vary the strength of each term relative to one another. Define the cost functional as

$$\mathcal{J}_\delta(\mathbf{u}, p, \underline{\sigma}, T, \tilde{g}) = \frac{a}{2} \int_{\Omega'} (\nabla \times \mathbf{u})^2 \, \mathrm{d}\Omega + \frac{\delta}{2} \int_{\Gamma_c} \tilde{g}^2 \mathrm{d}\Gamma + \frac{1-a}{2} \int_{\Gamma_{\text{out}}} \left(T - T^*\right)^2 \mathrm{d}\Gamma, \tag{14}$$

where $0 \leq a \leq 1$. Notice that in the first term on the right-hand side, we only integrate over a portion of the domain $\Omega' \subset \Omega$. The penalty term has a coefficient δ, which is assumed to be small.

Our optimal control problem is then to find a suitable control $\tilde{g}$ such that $\mathcal{J}_\delta$ is minimized subject to the state equation (5)–(12).

We will consider adjoint-based optimization techniques. Adjoint-based optimization methods turn a constrained optimization problem into an unconstrained one [13]. For completeness, we present the strong form of the adjoint equations, their boundary conditions, and the optimality condition. Motivation for the derivation of the equations and boundary conditions is given in the next section. The adjoint equations are:

$$\underline{\gamma} + d(\boldsymbol{\mu}) = \underline{0}, \tag{15}$$

$$2\nabla \cdot (\alpha \eta(T) \underline{\gamma}) - 2\nabla \cdot ((1-\alpha)\eta(T) d(\boldsymbol{\mu})) + \nabla \xi + \nabla T \Phi = -a \nabla \times \nabla \times \mathbf{u}, \tag{16}$$

$$\nabla \cdot \boldsymbol{\mu} = 0, \tag{17}$$

$$-\nabla \cdot (\kappa \nabla \Phi) - \mathbf{u} \cdot \nabla \Phi + \frac{2B}{T^2} \alpha \eta(T) \mathrm{d}(\mathbf{u}) : \underline{\gamma} - \frac{2B}{T^2} (1-\alpha) \eta(T) \mathrm{d}(\mathbf{u}) : \mathrm{d}(\boldsymbol{\mu}) = 0, \tag{18}$$

where $\underline{\gamma}$, $\boldsymbol{\mu}$, ξ, and Φ are the adjoint stress, velocity, pressure, and temperature, respectively. Note that the adjoint equations are linear in the adjoint variables.

The boundary conditions for the adjoint equations are as follows:

$$\boldsymbol{\mu} = \mathbf{0}, \qquad \Phi = 0 \quad \text{on } \Gamma_{\text{in}},$$

$$\boldsymbol{\mu} = \mathbf{0}, \qquad \frac{2B}{T^2}(1-\alpha)\eta(T)d(\mathbf{u})\cdot\boldsymbol{\mu}\cdot\mathbf{n} + \kappa\nabla\Phi\cdot\mathbf{n} = 0 \quad \text{on } \Gamma_{\text{wall}}\cup\Gamma_c,$$

$$\boldsymbol{\mu} = \mathbf{0}, \qquad \frac{2B}{T^2}(1-\alpha)\eta(T)d(\mathbf{u})\cdot\boldsymbol{\mu}\cdot\mathbf{n} + \kappa\nabla\Phi\cdot\mathbf{n} + \Phi\mathbf{u}\cdot\mathbf{n} + (1-a)(T-T^*) = 0 \quad \text{on } \Gamma_{\text{out}},$$

$$\boldsymbol{\mu}\cdot\mathbf{n} = \mathbf{0}, \qquad \frac{2B}{T^2}(1-\alpha)\eta(T)d(\mathbf{u})\cdot\boldsymbol{\mu}\cdot\mathbf{n} + \kappa\nabla\Phi\cdot\mathbf{n} = 0 \quad \text{on } \Gamma_{\text{sym}}.$$

Finally, the optimality condition is found to be

$$\tilde{g} + \frac{1}{\delta}\Phi = 0.$$

4. Variational formulation and finite element approximation

We develop the variational formulation of the modified non-isothermal Stokes–Oldroyd equations and the associated adjoint equations. Let $H^m(\Omega)$ be the standard Hilbert space with respect to a domain Ω and let $\|\cdot\|_m$ be the norm for $H^m(\Omega)$. We use $(\cdot,\cdot)_\Omega$ as the L^2 inner product for functions on Ω. Finally, let $\mathbf{H}^m(\Omega)$ be the corresponding Sobolev space of vector-valued functions in $\mathbb{R}^n$. We have the following approximation spaces for velocity, pressure, stress, and temperature, respectively:

$$\mathbf{X} := \{\mathbf{u}\in\mathbf{H}^1(\Omega) : \mathbf{u} = \mathbf{0} \text{ on } \Gamma_{\text{wall}}\cup\Gamma_c,\ \mathbf{u}\cdot\mathbf{n} = 0 \text{ on } \Gamma_{\text{sym}}\},$$

$$P := \left\{q\in L^2(\Omega) : \int_\Omega q\,\mathrm{d}\Omega = 0\right\},$$

$$\boldsymbol{\Sigma} := \left(L^2(\Omega)\right)^{n\times n}\cap\{\underline{\tau} = (\tau_{ij}) : \tau_{ij} = \tau_{ji},\ \tau_{ij}\in L^2(\Omega)\},$$

$$E := H^1(\Omega).$$

Notice that the velocity and pressure spaces, $\mathbf{X}$ and P, satisfy the inf–sup condition, [14,15]:

$$\inf_{q\in P}\sup_{\mathbf{v}\in\mathbf{X}}\frac{(q,\nabla\cdot\mathbf{v})_\Omega}{\|q\|_0\|\mathbf{v}\|_1} \geq \beta > 0.$$

Boundary functions in (9) and (11) are in $\mathbf{H}^{1/2}(\Gamma_{\text{in}})$ and $\mathbf{H}^{1/2}(\Gamma_{\text{out}})$, respectively.

For the weak formulation we also define test spaces:

$$\overline{\mathbf{X}} := \{\mathbf{v}\in\mathbf{H}^1(\Omega) : \mathbf{v} = \mathbf{0} \text{ on } \Gamma\setminus\Gamma_{\text{sym}},\ \mathbf{v}\cdot\mathbf{n} = 0 \text{ on } \Gamma_{\text{sym}}\},$$

$$\overline{E} := \{S\in H^1(\Omega) :\ S = 0 \text{ on } \Gamma_{\text{in}}\}.$$

Then the weak formulation for the system (5)–(8) is to find $(\mathbf{u}, p, \underline{\sigma}, T)\in\mathbf{X}\times P\times\boldsymbol{\Sigma}\times E$ so that

$$(\underline{\sigma},\underline{\tau})_\Omega - 2(\alpha\eta(T)d(\mathbf{u}),\underline{\tau})_\Omega = 0 \quad \forall\underline{\tau}\in\boldsymbol{\Sigma}, \tag{19}$$

$$(\underline{\sigma},\mathrm{d}(\mathbf{v}))_\Omega + 2((1-\alpha)\eta(T)\mathrm{d}(\mathbf{u}),d(\mathbf{v}))_\Omega - (p,\nabla\cdot\mathbf{v})_\Omega + ((pI-\underline{\sigma}+2(1-\alpha)\eta(T)d(\mathbf{u}))\cdot\mathbf{n},\mathbf{v})_{\Gamma_{\text{sym}}} = (\mathbf{f},\mathbf{v})_\Omega \quad \forall\mathbf{v}\in\mathbf{X}, \tag{20}$$

$$(q,\nabla\cdot\mathbf{u})_\Omega = 0 \quad \forall q\in P, \tag{21}$$

$$\kappa(\nabla T,\nabla S)_\Omega + (\mathbf{u}\cdot\nabla T,S)_\Omega - \kappa(\nabla T\cdot\mathbf{n},S)_{\Gamma_c} = (Q,S)_\Omega \quad \forall S\in E, \tag{22}$$

and the corresponding boundary conditions (9)–(12) are satisfied. The heat flux $\kappa(\nabla T\cdot\mathbf{n},S)_{\Gamma_c}$ arises from Green's theorem when obtaining the weak form of the energy equation. If the heat flux on Γ_c is given as

$$\tilde{g} = -\kappa\nabla T\cdot\mathbf{n}, \tag{23}$$

with $\tilde{g}\in\mathbf{L}^2(\Gamma_c)$, then the weak form of the energy equation becomes

$$\kappa(\nabla T,\nabla S)_\Omega + (\mathbf{u}\cdot\nabla T,S)_\Omega = (Q,S)_\Omega - (\tilde{g},S)_{\Gamma_c} \quad \forall S\in E. \tag{24}$$

We now present the motivation for the adjoint equations. We will describe the general framework and then apply it to our problem. Let ϕ denote the state variables, g the control variable(s), $F(\phi,g)$ the state equations, $\mathcal{J}$ the cost functional, and ζ the adjoint variables. The Lagrangian is defined as

$$\mathcal{L}(\phi,g,\zeta) = \mathcal{J} - \zeta^* F(\phi,g).$$

Then the unconstrained optimization problem is to find states ϕ, control g, and adjoint variables ζ so that the Lagrangian is rendered stationary. The first order necessary conditions yield the optimality system from which we can determine the optimal states ϕ and control g. Consider taking the Fréchet derivative with respect to the state variables, adjoint variables, and control. We then have the following relationships:

$$\frac{\partial \mathcal{L}}{\partial \phi} = 0 \Rightarrow \text{ Adjoint equations,}$$
$$\frac{\partial \mathcal{L}}{\partial \zeta} = 0 \Rightarrow \text{ State equations,}$$
$$\frac{\partial \mathcal{L}}{\partial g} = 0 \Rightarrow \text{ Optimality condition}(s).$$

With $\mathcal{J} = \mathcal{J}_\delta$ in (14), F as in (5)–(8) and the Dirichlet boundary conditions for the state equations, the Lagrangian is the following equation:

$$\begin{aligned}\mathcal{L}(\mathbf{u}, p, \underline{\sigma}, T, \tilde{g}, \boldsymbol{\mu}, \xi, \underline{\gamma}, \Phi, \rho, \lambda_i) = {} & \frac{a}{2}\int_{\Omega'} (\nabla \times \mathbf{u})^2 \, \mathrm{d}\Omega + \frac{\delta}{2}\int_{\Gamma_c} \tilde{g}^2 \mathrm{d}\Gamma \\ & + \frac{1-a}{2}\int_{\Gamma_{\text{out}}} (T - T^*)^2 \mathrm{d}\Gamma + \int_\Omega \left[\underline{\sigma} - 2\alpha\eta(T) d(\mathbf{u})\right] : \underline{\gamma} \, \mathrm{d}\Omega \\ & + \int_\Omega \left[-\nabla \cdot \left(\underline{\sigma} + 2(1-\alpha)\eta(T) d(\mathbf{u})\right) + \nabla p - \mathbf{f}\right] \cdot \boldsymbol{\mu} \, \mathrm{d}\Omega \\ & + \int_\Omega (-\nabla \cdot \mathbf{u}) \xi \, \mathrm{d}\Omega + \int_\Omega \left[-\nabla \cdot (\kappa \nabla T) + \mathbf{u} \cdot \nabla T - Q\right] \Phi \, \mathrm{d}\Omega \\ & + \int_{\Gamma_c} \tilde{g} \Phi \, \mathrm{d}\Gamma + \int_{\Gamma_{\text{in}}} (\mathbf{u} - \mathbf{u}_{\text{in}}) \lambda_1 \mathrm{d}\Gamma + \int_{\Gamma_{\text{wall}} \cup \Gamma_c} (\mathbf{u} - \mathbf{0}) \lambda_2 \mathrm{d}\Gamma \\ & + \int_{\Gamma_{\text{sym}}} (\mathbf{u} \cdot \mathbf{n} - 0) \lambda_3 \mathrm{d}\Gamma + \int_{\Gamma_{\text{in}}} (T - T_0) \lambda_4 \mathrm{d}\Gamma + \int_{\Gamma_{\text{out}}} (\mathbf{u} - \mathbf{u}_{\text{out}}) \lambda_5 \mathrm{d}\Gamma,\end{aligned}$$

where the λ_i's are the Lagrange multipliers associated with the boundary conditions. Taking the Fréchet derivative of the Lagrangian with respect to the state variables, and then applying Green's theorem will result in the weak form of the adjoint equations and their boundary conditions. Enforcing the domain integrals to be zero will yield the adjoint equations, and enforcing the boundary integrals to be zero will yield their boundary conditions. In particular, setting $\frac{\partial \mathcal{L}}{\partial \underline{\sigma}} = 0$ will yield the adjoint constitutive equation:

$$(\underline{\gamma}, \underline{\tau})_\Omega + (d(\boldsymbol{\mu}), \underline{\tau})_\Omega = 0 \quad \forall \underline{\tau} \in \boldsymbol{\Sigma}.$$

Taking the derivative of the Lagrangian with respect to velocity will give the adjoint momentum equation:

$$\begin{aligned}& -2(\alpha\eta(T)\underline{\gamma}, d(\mathbf{v}))_\Omega + 2((1-\alpha)\eta(T) d(\boldsymbol{\mu}), d(\mathbf{v}))_\Omega \\ & \quad -(\xi, \nabla \cdot \mathbf{v})_\Omega + (\mathbf{v} \cdot \nabla T, \Phi)_\Omega = -a(\nabla \times \mathbf{u}, \nabla \times \mathbf{v})_{\Omega'} \quad \forall \mathbf{v} \in \overline{\mathbf{X}}.\end{aligned}$$

The adjoint incompressibility condition is obtained by setting $\frac{\partial \mathcal{L}}{\partial p} = 0$:

$$(q, \nabla \cdot \boldsymbol{\mu})_\Omega = 0 \quad \forall q \in P.$$

Finally, taking the derivative with respect to temperature gives the adjoint energy equation:

$$\begin{aligned}& \kappa(\nabla \Phi, \nabla S)_\Omega - (\mathbf{u} \cdot \nabla \Phi, S)_\Omega + \left(2\frac{B}{T^2}\alpha\eta(T) d(\mathbf{u}) : \underline{\gamma}, S\right)_\Omega - \left(2\frac{B}{T^2}(1-\alpha)\eta(T) d(\mathbf{u}) : d(\boldsymbol{\mu}), S\right)_\Omega \\ & \quad = -(1-a)((T - T^*), S)_{\Gamma_{\text{out}}} \quad \forall S \in \overline{E}.\end{aligned}$$

The weak form of the optimality condition is found by setting $\frac{\partial \mathcal{L}}{\partial \tilde{g}} = 0$. We obtain

$$(\tilde{g}, S)_{\Gamma_c} = -\frac{1}{\delta}(\Phi, S)_{\Gamma_c},$$

for all $S \in H^1(\Gamma)$.

We will use the finite element method to approximate the solution to the state equations (19)–(21) and (24) and the adjoint equations. Suppose T_h is a triangulation of the domain Ω such that $\bar{\Omega} = \{\cup K : K \in T_h\}$; i.e., K is an element of the triangulation. Further suppose that there exist positive constants c_1 and c_2 such that

$$c_1 h \leq h_K \leq c_2 \rho_K,$$

where h_K is the diameter of K, ρ_K is the diameter of the greatest ball included in K, and $h = \max_{K \in T_h} h_K$. Denote the space of polynomials of degree less than or equal to k on $K \in T_h$ by $P_k(K)$. To approximate the solution $(\mathbf{u}, p, \underline{\sigma}, T)$, we define the following finite element spaces in $\mathbb{R}^2$.

$$\mathbf{X}^h := \{\mathbf{v} \in \mathbf{X} \cap (C^0(\bar{\Omega}))^2 : \mathbf{v}|_K \in P_2(K), \forall K \in T_h\},$$
$$P^h := \{q \in P \cap C^0(\bar{\Omega}) : q|_K \in P_1(K), \forall K \in T_h\},$$
$$\mathbf{\Sigma}^h := \{\underline{\tau} \in \mathbf{\Sigma} : \underline{\tau}|_K \in P_1(K), \forall K \in T_h\},$$
$$E^h := \{S \in E \cap C^0(\bar{\Omega}) : S|_K \in P_2(K), \forall K \in T_h\},$$
$$\overline{\mathbf{X}}^h := \{\mathbf{v} \in \overline{\mathbf{X}} \cap (C^0(\bar{\Omega}))^2 : \mathbf{v}|_K \in P_2(K), \forall K \in T_h\},$$
$$\overline{E}^h := \{S \in \overline{E} \cap C^0(\bar{\Omega}) : S|_K \in P_2(K), \forall K \in T_h\}.$$

We are using continuous piecewise quadratic elements for velocity and temperature, continuous piecewise linear elements for pressure, and discontinuous piecewise linear elements for stress. We use discontinuous elements in anticipation of applying this method to equations with more complex constitutive models which require a form of upwinding in the numerical approximation [16]. Analogous to the continuous function spaces, the discrete spaces $\mathbf{X}^h$ and P^h satisfy the discrete inf–sup condition [15]:

$$\inf_{q^h \in P^h} \sup_{\mathbf{v}^h \in \mathbf{X}^h} \frac{b(q^h, \mathbf{v}^h)_\Omega}{\|q^h\|_0 \|\mathbf{v}^h\|_1} \geq \beta > 0.$$

Then our discrete problem for the state variables is to find $(\mathbf{u}^h, p^h, \underline{\sigma}^h, T^h) \in (\mathbf{X}^h, P^h, \mathbf{\Sigma}^h, E^h)$ such that

$$(\underline{\sigma}^h, \underline{\tau}^h)_\Omega - 2(\alpha\eta(T^h)d(\mathbf{u}^h), \underline{\tau}^h)_\Omega = 0 \quad \forall \underline{\tau}^h \in \mathbf{\Sigma}^h, \tag{25}$$

$$(\underline{\sigma}^h, d(\mathbf{v}^h))_\Omega + 2((1-\alpha)\eta(T^h)d(\mathbf{u}^h), d(\mathbf{v}^h))_\Omega + ((p^h I - \underline{\sigma}^h + 2(1-\alpha)\eta(T^h)d(\mathbf{u}^h)) \cdot \mathbf{n}, \mathbf{v}^h)_{\Gamma_{\text{sym}}}$$
$$- (p^h, \nabla \cdot \mathbf{v}^h)_\Omega = (\mathbf{f}, \mathbf{v}^h)_\Omega \quad \forall \mathbf{v}^h \in \overline{\mathbf{X}}^h, \tag{26}$$

$$(q^h, \nabla \cdot \mathbf{u}^h)_\Omega = 0 \quad \forall q^h \in P^h, \tag{27}$$

$$\kappa(\nabla T^h, \nabla S^h)_\Omega + (\mathbf{u}^h \cdot \nabla T^h, S^h)_\Omega = (Q, S^h)_\Omega - (\tilde{g}, S^h)_{\Gamma_c} \quad \forall S^h \in \overline{E}^h, \tag{28}$$

and the corresponding boundary conditions are satisfied. Similarly, the discrete problem for the adjoint variables is to find $(\boldsymbol{\mu}^{(h)}, \xi^h, \underline{\gamma}^h, \Phi^h) \in (\overline{\mathbf{X}}^h, P^h, \mathbf{\Sigma}^h, \overline{E}^h)$ such that

$$(\underline{\gamma}^h, \underline{\tau}^h)_\Omega + (d(\boldsymbol{\mu}^{(h)}), \underline{\tau}^h)_\Omega = 0 \quad \forall \underline{\tau}^h \in \mathbf{\Sigma}^h, \tag{29}$$

$$-2(\alpha\eta(T^h)\underline{\gamma}^h, d(\mathbf{v}^h))_\Omega + 2((1-\alpha)\eta(T^h)d(\boldsymbol{\mu}^{(h)}), d(\mathbf{v}^h))_\Omega - (\xi^h, \nabla \cdot \mathbf{v}^h)_\Omega + (\mathbf{v}^h \cdot \nabla T^h, \Phi^h)_\Omega$$
$$= -a(\nabla \times \mathbf{u}^h, \nabla \times \mathbf{v}^h)_{\Omega'} \quad \forall \mathbf{v}^h \in \overline{\mathbf{X}}^h, \tag{30}$$

$$(q^h, \nabla \cdot \boldsymbol{\mu}^{(h)})_\Omega = 0 \quad \forall q^h \in P^h, \tag{31}$$

$$\kappa(\nabla \Phi^h, \nabla S^h)_\Omega - (\mathbf{u}^h \cdot \nabla \Phi^h, S^h)_\Omega + 2\left(\frac{B}{(T^h)^2}\alpha\eta(T^h)d(\mathbf{u}^h) : \underline{\gamma}^h, S^h\right)_\Omega$$
$$- 2\left(\frac{B}{(T^h)^2}(1-\alpha)\eta(T^h)d(\mathbf{u}^h) : d(\boldsymbol{\mu}^{(h)}), S^h\right)_\Omega = -(1-a)(T^h - T^*, S^h)_{\Gamma_{\text{out}}} \quad \forall S^h \in \overline{E}^h, \tag{32}$$

and the corresponding boundary conditions are satisfied.

To solve the unconstrained optimization problem, we use the method of steepest descent [13]. The gradient method step is

$$\tilde{g}^{(n+1)} = \tilde{g}^{(n)} - \frac{\nu}{\delta}\frac{\partial \mathcal{J}_\delta}{\partial \tilde{g}},$$

where δ is the penalty parameter in the functional (14) and $\frac{\nu}{\delta}$ is a (constant) step size. By calculating $\frac{\partial \mathcal{J}_\delta}{\partial \tilde{g}}$, we find that the update for the control $\tilde{g}$ is

$$\tilde{g}^{(n+1)} = (1-\nu)\tilde{g}^{(n)} - \frac{\nu}{\delta}\Phi^{(n)}.$$

We will use the following steps when solving the optimal control problem. Initialize the control variable $\tilde{g}^{(0)}$. For $n = 0, 1, \ldots$

1. Solve the state equations to obtain the state solution $(\mathbf{u}^{(n)}, p^{(n)}, \underline{\sigma}^{(n)}, T^{(n)})$.
2. Solve the adjoint equations to obtain the adjoint solution $(\boldsymbol{\mu}^{(n)}, \xi^{(n)}, \underline{\gamma}^{(n)}, \Phi^{(n)})$.
3. Evaluate the cost functional $\mathcal{J}_\delta(\mathbf{u}^{(n)}, p^{(n)}, \underline{\sigma}^{(n)}, T^{(n)}, \tilde{g}^{(n)})$ (optional).
4. Update the control via $\tilde{g}^{(n+1)} = (1-\nu)\tilde{g}^{(n)} + \frac{\nu}{\delta}\Phi^{(n)}$.

Table 1
Parameter values.

α	A	B	δ
$\frac{1}{2}$	1.0×10^{-14}	14,500	0.00005

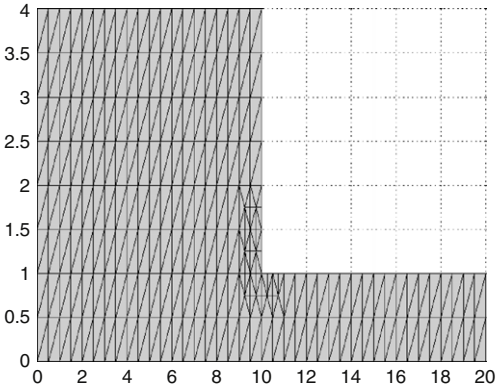

Fig. 4. Computational mesh used for the FEM.

5. Test for convergence, either by checking the optimality condition $\tilde{g}^{(n)} + \frac{1}{\delta}\Phi^{(n)} = 0$, or a maximum change in the control $\|\tilde{g}^{(n+1)} - \tilde{g}^{(n)}\|_\infty$.
6. Repeat all steps until convergence is attained.

Newton's method is used in Step 1 due to the nonlinear forms present in the state system. The step size $\frac{\nu}{\delta}$ for the gradient method is chosen appropriately so that a favorable convergence in the iterates is observed. A more rigorous method for determining the step size, including adaptivity, would improve convergence properties. Such an approach is beyond the scope of the current work.

5. Numerical results

In this section, we consider three scenarios: the problems of vortex minimization and temperature matching, and the combination of those two problems. In all three problems, we have the following characteristics. The dimensions of the channel before the contraction are $\{(x, y) : 0 \leq x \leq 10, 0 \leq y \leq 4\}$, while after the contraction the dimensions become $\{(x, y) : 10 \leq x \leq 20, 0 \leq y \leq 1\}$. The computational mesh is shown in Fig. 4. A more refined mesh was considered, but it was found that the solution is not appreciably affected. Recall that the cost functional has the form (14), where $\Omega' \subset \Omega$ and $a \in [0, 1]$. The boundary segments that comprise Γ_c were determined so that the vortex is contained within the rectangle defined by these boundary segments. For the conditions in this work, it sufficed to let $\Gamma_c = \{(x, y)|8 \leq x \leq 10, y = 4\} \cup \{(x, y)|x = 10, 2.5 \leq y \leq 4\}$. The region Ω' is $\{(x, y) : 8 \leq x \leq 10, 2.5 \leq y \leq 4\}$. Both the state pressure p and the adjoint pressure ξ are only determined up to a constant. We assume that the desired temperature T^* is constant along Γ_{out}. For future reference, define the quadratic forms $\mathcal{J}_1$ and $\mathcal{J}_2$ as

$$\mathcal{J}_1 = \frac{a}{2}\int_{\Omega'} (\nabla \times \mathbf{u})^2 \, \mathrm{d}\Omega,$$
$$\mathcal{J}_2 = \frac{1-a}{2}\int_{\Gamma_{\text{out}}} (T - T^*)^2 \mathrm{d}\Gamma.$$

5.1. Vortex minimization

We will consider the problem of minimizing the vortex in the four-to-one contraction domain. Here we consider the case where $a = 1$, i.e., we concentrate on minimizing the vortex and ignore matching the temperature along Γ_{out}. In this and all subsequent examples we set the source terms $\mathbf{f}$ and Q to zero, and assign the other parameter values as given in Table 1. For this first case, we set

$$\nu = 0.05.$$

The values for A and B lead to typical zero-shear viscosity profiles for $\eta(T)$ [10]. Also, notice that the step size for the gradient method is $\frac{\nu}{\delta} = 1000$. The optimal control code ran for 153 iterations before the convergence criterion was met. The results of the run are summarized in Table 2. We are able to reduce the vortex by controlling the heat flux across the boundary. We

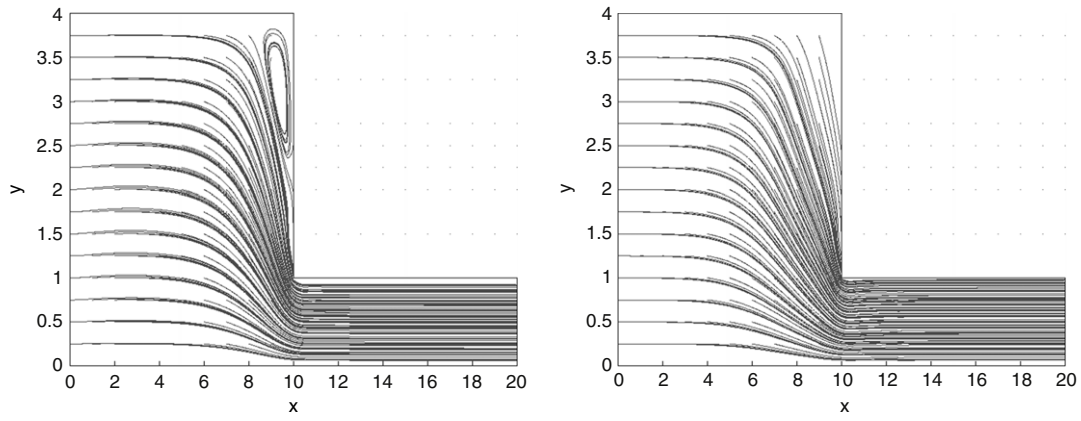

(a) Uncontrolled flow. (b) Controlled flow.

Fig. 5. Comparison of streamlines after 153 iterations of the control algorithm.

Table 2
Results of the vortex minimization run.

Iteration	$\mathcal{I}_1$
1	1.2667
2	1.2220
3	1.1750
4	1.1268
5	1.0780
6	1.0290
7	0.9796
8	0.9288
9	0.8747
10	0.8147
11	0.7462
12	0.6695
⋮	⋮
151	0.2461
152	0.2461
153	0.2461

can also compare plots of the streamlines for the uncontrolled and controlled flows. These are shown in Fig. 5. We are able to reduce the value of the integral by 80.6%, and it is apparent from these plots that the remaining vortex is significantly weaker than in the uncontrolled flow.

Recall that the control affects the solution of the state equations through the addition of the inner product $-(\tilde{g}, S)_{\Gamma_c}$ in the energy equation. Hence, a positive value for $\tilde{g}$ yields a heat sink along Γ_c, and a negative value of $\tilde{g}$ yields a heat source along Γ_c. We see that we need to cool on Γ_c to reduce the vortex. Fig. 6 contains the profile of $\tilde{g}$ as computed in this example.

5.2. Temperature matching

Now we consider the case when $a = 0$, or we simply would like to match a desired temperature T^* at the outflow boundary Γ_{out}. For this run, we set $\nu = 0.005$. Here notice that the step size for the gradient method is $\frac{\nu}{\delta} = 100$. Furthermore, we decide to match a desired temperature of $T^* = 550$ K from an initial temperature of $T_0 = 540$ K. Define $\bar{T}_f$ to be the nodal average of T along Γ_{out}. The results are in Table 3. The integral $\mathcal{I}_2$ strictly decreases, which means that as we iterate, we get closer to matching T^* along Γ_{out}. We may also consider the profile of the control $\tilde{g}$. The computed control is presented in Fig. 7. The negative values of $\tilde{g}$ mean that we heat along Γ_c. The heating in this case tends to increase the magnitude of the vortex. In this case, the quadratic form $\mathcal{I}_1$ will increase due to the addition of heat.

5.3. Combination of problems

We have shown that we are able to minimize the vortex and match a desired outflow temperature separately. In this section we attempt to minimize both subfunctionals at the same time. Thus, we let $a = \frac{1}{2}$. We consider the case where the matching temperature is smaller than the temperature on the inflow boundary, i.e., $T^* < T_0$. For this case,

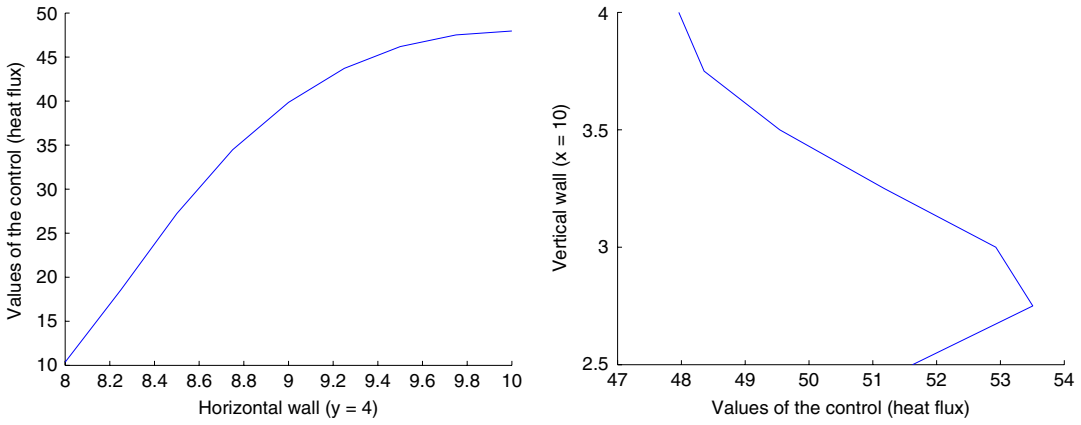

(a) Horizontal wall. (b) Vertical wall.

Fig. 6. Profile of the control $\tilde{g}$.

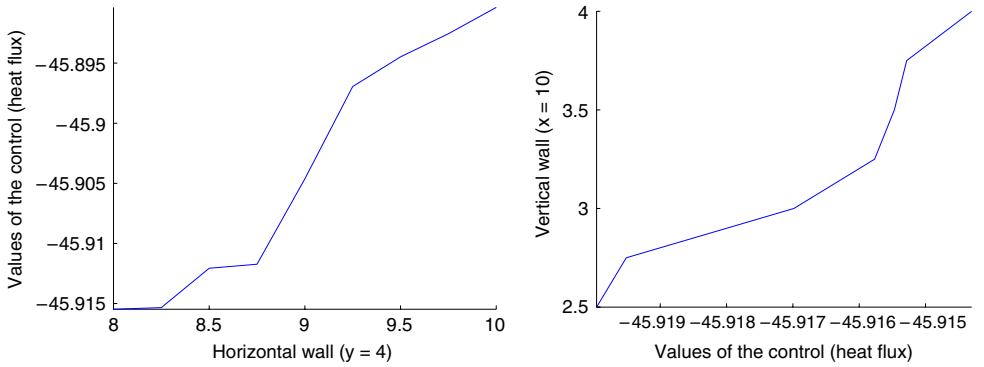

(a) Horizontal wall. (b) Vertical wall.

Fig. 7. Profile of the control $\tilde{g}$ for the temperature matching case.

$\nu = 0.0025,$
$T^* = 530,$
$T_0 = 540.$

The step size for the gradient method is $\frac{\nu}{\delta} = 50$. We summarize the results by displaying the first seven iterates in Table 4. We are able to minimize both subfunctionals $\mathcal{J}_1$ and $\mathcal{J}_2$. In order to match the desired temperature, we are required to remove heat through Γ_c which in turn reduces the vortex. The profiles of the control $\tilde{g}$ along the horizontal and vertical walls for this case are presented in Fig. 8.

6. Conclusions and future work

The main thrust of this research is to apply optimal control techniques to equations modeling non-isothermal viscous flow in four dependent variables. Specifically, we considered fluid flow through a four-to-one contraction domain, where a vortex is generated near the corner region of the contraction. Within this vortex, the fluid will recirculate for some time before being released, and may degrade. This leads to an inferior product upon extrusion. In addition to the vortex minimization problem, we looked at temperature matching along the outflow boundary. The control in each case was the heat flux across the boundary in the corner region. For the single problem of vortex minimization, we found that a combination of heating and cooling reduces the vortex. For the separate problem of temperature matching, we were able to match a specified outflow temperature T^* from an initial temperature of T_0.

We then considered a combination of the problems. We found that we are able to minimize both the vortex and the temperature difference along the outflow boundary in the case where $T^* < T_0$. This was attained by removing heat from the system along the control boundary Γ_c.

There are many directions that we could pursue based upon this research. The first is to move on to non-Newtonian constitutive models. Recall that the modified non-isothermal Stokes–Oldroyd equations were designed with the ultimate goal of implementing a viscoelastic constitutive model in mind. In turn, we could also progress to three-dimensional flows.

Table 3
Results of the temperature matching run.

Iteration	$\mathcal{I}_2$	$\bar{T}_f$
1	50.0	540.0
2	6.39	553.57
3	0.92	548.64
4	0.10	550.44
5	0.02	549.79
6	3.55×10^{-4}	550.03
7	1.79×10^{-3}	549.94
8	4.13×10^{-4}	549.97
9	7.99×10^{-4}	549.96
10	6.44×10^{-4}	549.96
11	6.98×10^{-4}	549.96
12	6.78×10^{-4}	549.96
13	6.86×10^{-4}	549.96
14	6.83×10^{-4}	549.96

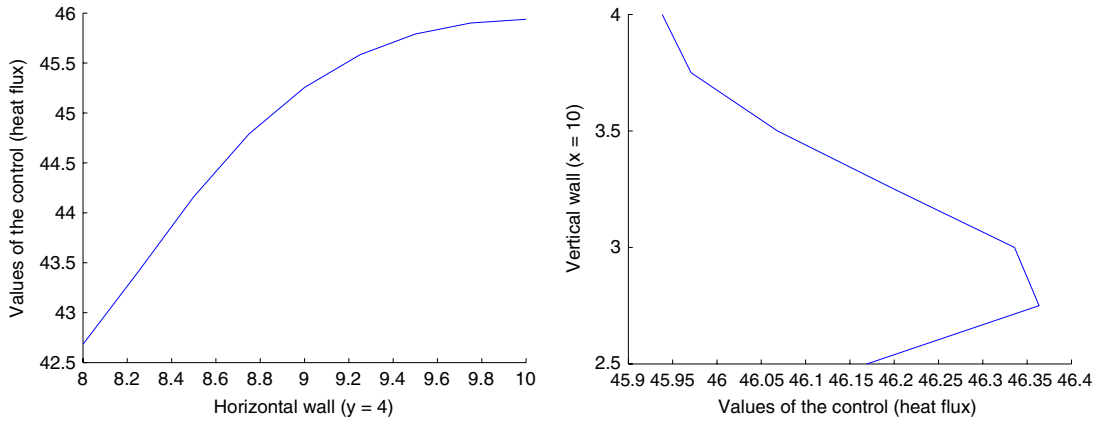

(a) Horizontal wall. (b) Vertical wall.

Fig. 8. Profile of the control $\tilde{g}$ for when $T^* < T_0$.

Table 4
Cost functional values for when $T^* < T_0$.

Iteration	$\mathcal{J}_\delta$	$\mathcal{I}_1$	$\mathcal{I}_2$
1	25.63	0.63	25.0
2	11.30	0.43	10.85
3	5.04	0.32	4.66
4	2.32	0.23	1.99
5	1.15	0.18	0.85
6	0.65	0.14	0.37
7	0.44	0.12	0.16

In addition to the increase in complexity of the equations and advancing in spatial dimension, there are a couple of other directions we could consider. As we have only considered the flow up to the extrusion point, it would be interesting to extend the domain to include the free surface region where the fluid cools and the draw ratio is large. Optimization and control for the problem of die swell is of strong interest to industry [17]. Other optimization problems could be considered as well, such as shape optimization, to determine an optimal geometry for the interior flow domain.

Acknowledgements

The authors gratefully acknowledge Patti Sylvia for programming assistance, and the reviewers of this manuscript for several valuable suggestions.

References

[1] D.V. Boger, Viscoelastic flows through contractions, Annual Review of Fluid Mechanics 19 (1987) 157–182.
[2] M.E. Kim-E, R.A. Brown, R.C. Armstrong, The roles of inertia and shear-thinning in flow of an inelastic liquid through an axisymmetric sudden contraction, Journal of Non-Newtonian Fluid Mechanics 13 (1983) 341–363.

[3] G.W.M. Peters, F.P.T. Baaijens, Modelling of non-isothermal viscoelastic flows, Journal of Non-Newtonian Fluid Mechanics 68 (1997) 205–224.
[4] K. Kunisch, X. Marduel, Optimal control of non-isothermal viscoelastic fluid flow, Journal of Non-Newtonian Fluid Mechanics 88 (2000) 261–301.
[5] K. Ito, S.S. Ravindran, Optimal control of thermally convected fluid flows, SIAM Journal of Scientific Computing 19 (6) (2000) 1847–1869.
[6] J. Baranger, D. Sandri, A formulation of Stoke's problem and the linear elasticity equations suggested by the Oldroyd model for viscoelastic flow, Mathematical Modelling and Numerical Analysis 26 (1992) 331–345.
[7] R.B. Bird, R.C. Armstrong, O. Hassager, Dynamics of Polymeric Liquids, vol. 1, John Wiley & Sons, 1987.
[8] P. Lomellini, Viscosity-temperature relationships of a polycarbonate melt: Williams–Landel–Ferry versus Arrhenius behaviour, Die Makromolekulare Chemie 193 (1992) 69–79.
[9] C.L. Cox, H.K. Lee, D.C. Szurley, Finite element approximation of the non-isothermal Stokes–Oldroyd equations, International Journal of Numerical Analysis and Modeling 4 (3–4) (2007) 425–440.
[10] Y.L. Joo, J. Sun, M.D. Smith, R.C. Armstrong, R.A. Brown, R.A. Ross, Two-dimensional numerical analysis of non-isothermal melt spinning with and without phase transition, Journal of Non-Newtonian Fluid Mechanics 102 (2002) 37–70.
[11] J.G. Heywood, R. Rannacher, S. Turek, Artificial boundaries and flux and pressure conditions for the incompressible Navier–Stokes equations, International Journal for Numerical Methods in Fluids 22 (5) (1996) 325–352.
[12] M.D. Gunzburger, L. Hou, T.P. Svobodny, Heating and cooling control of temperature distributions along boundaries of flow domains, Journal of Mathematical Systems, Estimation, and Control 3 (2) (1993) 147–172.
[13] M.S. Bazaraa, H.D. Sherali, C.M. Shetty, Nonlinear Programming, John Wiley & Sons, 1993.
[14] S.C. Brenner, L.R. Scott, The Mathematical Theory of Finite Element Methods, Springer-Verlag, 1996.
[15] V. Girault, P.-A. Raviart, Finite Element Approximation of the Navier–Stokes Equations, Springer-Verlag, 1979.
[16] F.P.T. Baaijens, An iterative solver for the DEVSS/DG method with application to smooth and non-smooth flows of the upper convected Maxwell fluid, Journal of Non-Newtonian Fluid Mechanics 75 (1998) 119–138.
[17] M.M. Denn, Issues in viscoelastic fluid mechanics, Annual Review of Fluid Mechanics 75 (1990) 13–34.